A New Compact Microstrip UWB Bandpass Filter with Triple-Notched Bands

Ruifang Su[1], Ting Luo[1, *], Wenlan Zhang[1], Junding Zhao[2], and Zifei Liu[3]

Abstract—A new compact microstrip UWB bandpass filter with triple band-notched characteristics is presented in this paper. The initial circuit topology and its corresponding electrical parameters of the basic microstrip UWB BPF are desired by a variation of genetic algorithm (GA) technique. Then, triple-notched bands inside the UWB passband are implemented by coupling a novel triple-mode stepped impedance resonator (TMSIR) to the main transmission line of the basic microstrip UWB BPF. The triple-notched bands can be easily generated and set at any desired frequencies by varying the designed parameters of TMSIR. To illustrate the possibilities of the new approach, a microstrip UWB BPF with triple-notched bands respectively centered at frequencies of 5.2 GHz, 6.8 GHz, and 8.0 GHz is designed and fabricated. Measured results agree well with the predicted counterparts.

1. INTRODUCTION

In February 2002, the U.S. Federal Communications Commission allocated 3.1–10.6 GHz band as unlicensed spectrum for ultra-wideband (UWB) systems [1]. An UWB BPF, as one of the essential components of the UWB systems, has gained much attention in recent years. There are many techniques presented to design UWB bandpass filters. For example, multiple-mode resonator (MMR) [2], multilayer coupled structure [3], defected ground structure (DGS) [4], and the cascaded low-pass/high-pass filters [5] have been widely used to achieve UWB characteristics.

However, the existing wireless networks such as 4.5G satellite communication systems signals, 5.8 GHz WLAN signals, and 6.8 GHz RF identification (RFID) communication systems signals can easily interfere with UWB users, therefore, compact UWB BPF with multiple notched bands is emergently required to reject these interfering signals [6–12]. To achieve a notched band, one of two arms in the coupled-line sections is extended and folded in [6]. On the other side, the coupling interdigital line is introduced to block undesired existing radio signals in [7]. However, these two methods can only achieve one notched band. Thus, to introduce dual notched bands, a coupled simplified composite right/left-handed resonator is introduced in [8] and two coupled stepped impedance resonators are employed in [9]. However, the selectivity designed with these two methods need to be improved. By arranging two asymmetric meander open-loop resonators on middle layer and a C-shaped resonator on bottom layer [10] or embedding two open-circuit stubs into broadside-coupled stepped impedance resonators on middle layer [11], dual notched bands can be introduced into an UWB BPF. Additionally, by integrating short-circuited stub resonators [12] or embedding a quarter-wavelength coplanar waveguide resonators and inserting a meander slot-line in the detached-mode resonator [13] can also realize dual notched bands. However, these designs are based on multilayer technology which will increase the fabrication cost. And a new method based on wave's cancellation theory has been proposed to design an UWB BPF with dual notched band in [14]. However, the center frequencies and bandwidths of the notched

bands can not be adjusted. Two tri-section stepped impedance resonators and a parallel gap-coupled microstrip resonator are used in [15] and two L-shaped folded shunt open-circuited stubs are placed on the feed lines in [16] to achieve triple notched bands. However, the performance of the filter is not ideal. Furthermore, design efficiencies of the filters mentioned above need to be improved.

In this paper, we present a novel compact microstrip UWB bandpass filter with triple band-notched characteristics. The basic microstrip UWB BPF is designed by a variation of genetic algorithm (GA) technique to simultaneously search for the appropriate circuit topology and its corresponding electrical parameters. By improving the fitness evaluation, selection, crossover, and mutation, we overcome the two possible drawbacks of conventional GA technique, i.e., slow rate of convergence and local-best solution, thus to achieve better accuracy and high efficiency for the basic UWB BPF design. Then, triple-notched bands property is achieved by coupling a novel triple-mode stepped impedance resonator (TMSIR) to the main transmission line. The triple-notched bands can be easily generated and realized by controlling the locations of even-odd modes resonance frequency of the TMSIR. The designed methodology is very efficient and useful for filter synthesis though the design principle is simple. Moreover, the structure is compact and the filter has good performance. Finally, the proposed filter is designed, fabricated and measured. Good agreement between measured and simulated results is achieved.

2. UWB BANDPASS FILTER DESIGN

An arbitrary two-port microstrip circuit shown in Fig. 1(a) can be decomposed into basic circuit elements [17, 18] shown in Fig. 1(b). The circuit can be expressed as a data structure shown in Fig. 1(c). The data structure is composed of three parts. The first part coded in integer represents the topology of basic element. The second part coded in integer represents the way of connection to the previous element. The third part coded in floating number represents the corresponding electrical parameters. In the GA, we define a basic circuit element as a gene and a set of basic circuit elements as a chromosome [19–21]. Therefore, an arbitrary two-port circuit can be represented by a chromosome. Table 1 is the details of the basic circuit elements. A special gene named *Empty* is introduced, which enables the representation scheme to be capable of describing a circuit with an arbitrary number of basic circuit elements and orders. In this work, we adopt a variation of GA technique to design a microstrip UWB BPF with improved design efficiency.
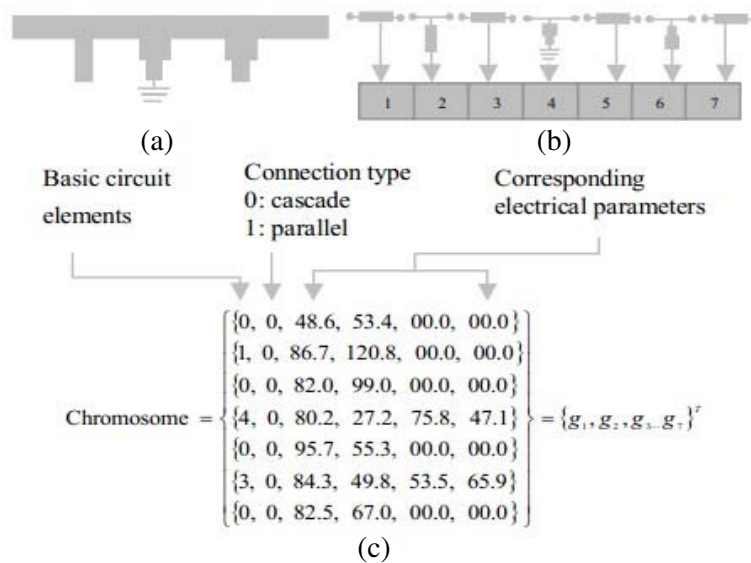

Figure 1. Representation scheme in the variation of genetic algorithm: (a) a typical microstrip circuit, (b) decomposition of the circuit in (a) into basic circuit elements, (c) chromosome of the circuit in (a).

Table 1. Details of the basic elements in the variation of genetic algorithm.

Category	Type	Name	Network Topology	Electrical Parameters			
	0	TL			Z_{01}	Z_{01}	
	1	Open			Z_{01}	Z_{01}	
Basic Circuit Elements	2	Short			Z_{01}	Z_{01}	
	3	SIR_Open		Z_{01}	Z_{01}	Z_{02}	θ_{02}
	4	SIR_Short		Z_{01}	Z_{01}	Z_{02}	θ_{02}
	5	Empty		0	0	0	0

2.1. Initialization

The initial population has an effect on the convergence, so we make every chromosome randomly initialize within the specific electrical parameters range of every basic element for better convergence in this scheme. What's more, it is necessary to assign upper and lower limits according to various designs and engineering requirements. Due to the tolerance of the fabrication, the minimum width is limited to 0.1 mm, which corresponds to a microstrip line with a characteristic impedance of 137 Ω. Meanwhile, to lower the junction discontinuity effects, the maximum line width is chosen to be 2 mm, which corresponds to a microstrip line with a characteristic impedance of 40 Ω.

2.2. Fitness Evaluation

The transmission-line models are used to calculate scattering parameters (S21) to effectively evaluate the frequency response of a chromosome. We make ABCD matrix multiplication as cascade no matter the basic element is in series or parallel connection. It should be mentioned that the gene named *Empty* represents unit matrix. The method will improve the calculation speed of procedures and efficiency of algorithm. The desired function is shown in Fig. 2 and the fitness value is defined by:
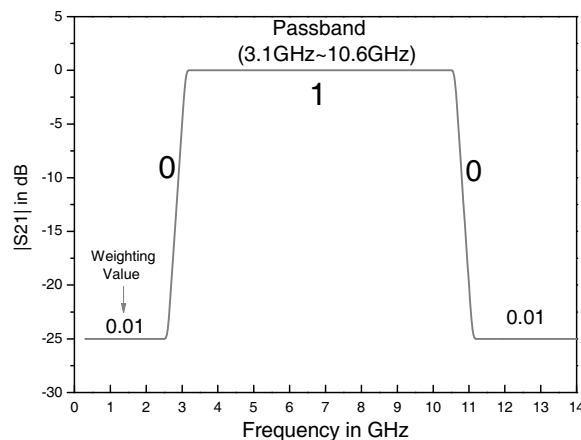
$$F = \sum_{i=1}^{N} w_i f_i \tag{1}$$

Figure 2. The desired function of the proposed basic UWB BPF.

where w_i represents the weighting value at the ith sampling point, f_i the square deviation between the calculated scattering parameter and the desired value at the ith sampling point, and N the number of sampling points.

2.3. Genetic Operator

Although the roulette wheel selection based on the proportionate selection is widely used in the GA, there is a drawback that the type of fitness function has an effect on the convergence. Thus, in this paper, the tournament selection is used.

Crossover operator is an important operator and it plays a decisive role in global convergence of the algorithm. The way of the crossover decides whether we can find the optimal solution and the speed of finding the optimal solution. Therefore, the scheme employs a high efficiency crossover method of combining bubble sort with single-point crossover.

Mutation as a reproduction operator has a key role of getting out from the trap of the local optimum solution and keeping the diversity of population. In this work, mutation is carried out to randomly alter the values of genes in a parent chromosome with probability.

2.4. Result and Performance

Here, an basic microstrip UWB BPF is desired by GA technique. The study is completed on a computer with a 2-GHz microprocessor, and the computing time of the example is only 1.8 min. For the design, the best chromosome after 18 generations consists of four empty element, five transmission lines, and four stubs. The proposed filter is realized on the substrate Duroid 5880 ($\varepsilon_r = 2.2$, $h = 0.508$, $\tan \delta = 0.003$). Table 2 lists the electrical and final physical parameters. It should be mentioned that the values in Table 2 are calculated by the following steps: Firstly, we transform the chain of ABCD matrix for the chromosome to the scattering matrix. Secondly, we search for the optimal solution by optimizing the topology and its corresponding electrical parameters according to the design specification shown in Fig. 2. Thirdly, we convert the achieved electrical parameters to original physical parameters according to the corresponding relationship. Finally, we construct the filter model in HFSS, i.e., the proposed basic UWB BPF layout in Fig. 3, according to the original physical parameters. Notice that we have slightly

Table 2. Electrical and physical parameters of the basic UWB BPF.

| No.	Name	Electrical Parameters (at $f_0 = 6.9$ GHz)				Physical Parameters in mm			
		z_{01}	θ_{01}	z_{02}	θ_{02}	W_{01}	L_{01}	W_{02}	L_{02}
1	Short	97.8	70.3	0	0	0.3	5.4	0	0
2	TL	52.2	47.8	0	0	1.1	3.5	0	0
3	Empty	0	0	0	0	0	0	0	0
4	TL	72.7	66.7	0	0	0.6	5	0	0
5	TL	67.3	71.0	0	0	0.7	5.3	0	0
6	Empty	0	0	0	0	0	0	0	0
7	SIR_Short	52.2	66.9	67.3	21.4	1.1	4.9	0.7	1.6
8	TL	58.6	74.3	0	0	0.9	5.5	0	0
9	Empty	0	0	0	0	0	0	0	0
10	Open	72.7	20.6	0	0	0.6	1.5	0	0
11	Empty	0	0	0	0	0	0	0	0
12	TL	72.9	37.3	0	0	0.6	2.8	0	0
13	SIR_Short	87.3	84.0	67.3	20.1	0.4	6.4	0.7	1.5
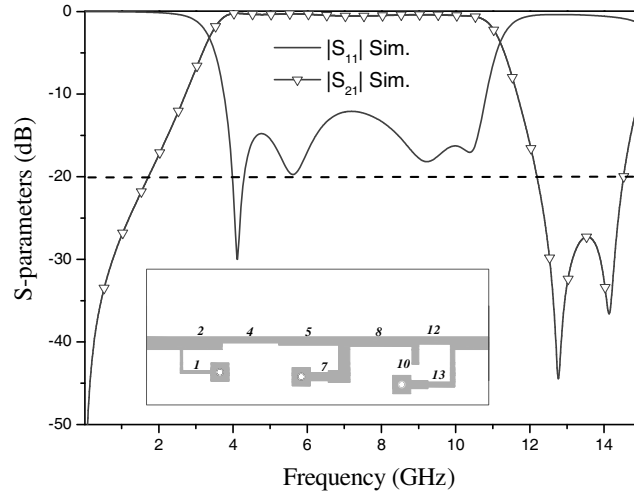
Figure 3. Simulated performance of proposed basic UWB BPF.

adjusted some initial physical parameters considering the discontinuity effects and fringing capacitances. The simulated scattering parameters are shown in Fig. 3. Referring to Fig. 3, the proposed UWB BPF has an insertion loss better than 3 dB over the 3.3–11.1 GHz bandwidth and the upper-stopband with -10 dB attenuation is up to 15 GHz. In addition, the return loss is under -15 dB over most part of the passband.

3. TRIPLE-MODE STEPPED IMPEDANCE RESONATOR ANALYSIS

To realize band-notched characteristics, we introduce a novel TMSIR into the basic UWB BPF. This structure is simple and flexible for blocking undesired narrow band radio signals that may appear in UWB band. Fig. 4(a) shows the geometry of the proposed TMSIR [22]. Since the resonator is symmetrical to the T-T' plane, the odd-even-mode method is implemented. For odd-mode excitation, the equivalent circuit is one quarter-wavelength resonator with one end grounded, as shown in Fig. 4(b). From the resonance condition of $Y_{\mathrm{ino}} = 0$, the odd-mode resonant frequency can be deduced as:

$$f_{notch-ino} = \frac{c}{4L_1\sqrt{\varepsilon_{eff}}} \tag{2}$$

where f_{ino} is the center frequency of the notch band, ε_{eff} the effective dielectric constant, and c the light speed in free space.

For even-mode excitation, the equivalent circuit is shown in Fig. 4(c), which contains two resonant circuits: a quarter-wave-length resonator and a half-wavelength resonator, as shown in Figs. 4(d) and 4(e). The even-mode resonant frequencies can be determined as follows:

$$f_{notch-ine1} = \frac{c}{4(L_1 + L_2 + L_3)\sqrt{\varepsilon_{eff}}} \tag{3}$$

$$f_{notch-ine2} = \frac{c}{(2L_1 + 2L_2 + 2L_4)\sqrt{\varepsilon_{eff}}} \tag{4}$$

where are $Z_1 = Z_3 = Z_4$ assumed for simplicity. The resonance frequencies can be determined by the electrical length. Compared with dual-mode resonator, the proposed structure can provide three resonant frequencies and higher degree of freedom in adjusting the locations of the resonant modes.

The TMSIR can result in triple band-stop performance when placed next to the microstrip line and it can be equivalent to three shunt-connected series resonance circuits, as shown in Fig. 5. The TMSIR can result in triple band-stop (i.e., the triple notched-bands) performance when placed next to the microstrip line and it can be equivalent to three shunt-connected series resonance circuits.
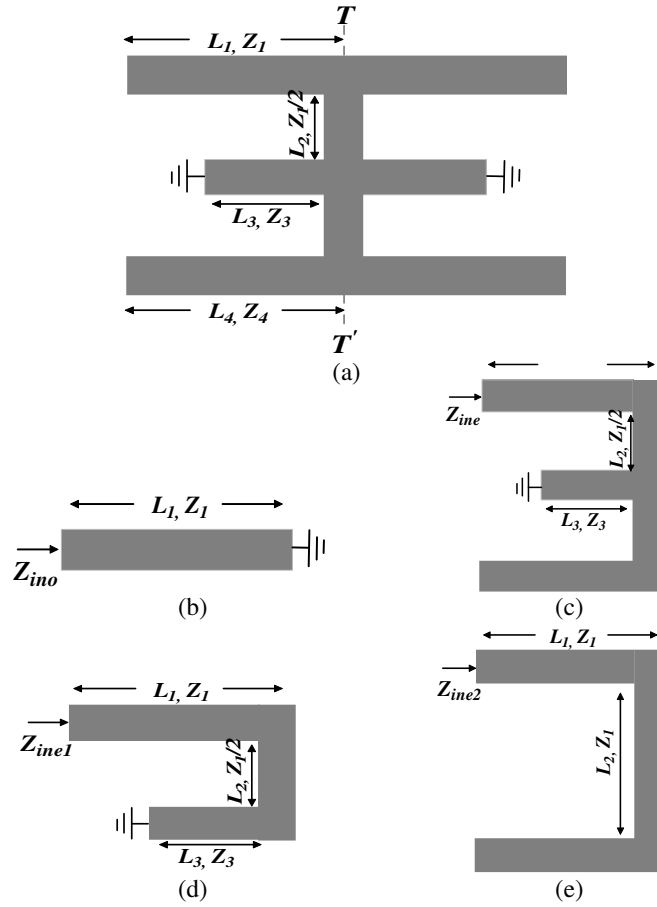
Figure 4. (a) Configuration of the proposed novel TMSIR, (b) Odd-mode equivalent circuit, (c) Even-mode equivalent circuit, (d) Path I of Even-mode equivalent circuit, (e) Path II of Even-mode equivalent circuit.

The bandwidth of the notched band can be controlled by tuning the coupling coefficient k_m of the coupled TMSIR as illustrated in Fig. 6. It should be mentioned that the coupling coefficient k_m is defined by:

$$k_m = \frac{f_{notch-ino}^2 - f_{notch-ine1}^2}{f_{notch-ino}^2 + f_{notch-ine1}^2} \tag{5}$$

Referring to Fig. 6(a), the coupling coefficient k_m decreases as increasing W_{gap}. Referring to Fig. 6(b), the stronger coupling between the TMSIR and the main transmission line is, the wider bandwidth of the notched band will be. Thus, the bandwidth of the notched band can be controlled by suitably shifting the coupling coefficient between the TMSIR and the main transmission line. In this paper, the coupling coefficient is selected $k_m = 0.442$ and the TMSIR dimensions are as follows: $w_{s1} = 1.3\,\text{mm}$, $w_{s2} = 0.3\,\text{mm}$, $w_{s3} = 0.3\,\text{mm}$, $w_{s5} = 1.3\,\text{mm}$, $l_{s1} = 4.5\,\text{mm}$, $l_{s2} = 0.5\,\text{mm}$, $l_{s3} = 1.45\,\text{mm}$, $l_{s4} = 0.7\,\text{mm}$, $l_{s5} = 3.1\,\text{mm}$, $l_{s6} = 1.6\,\text{mm}$, $r_e = 0.1\,\text{mm}$, $w_{gap} = 0.1\,\text{mm}$.

The frequency characteristics of the coupled TMSIR with various dimensions are investigated by HFSS 11.0 to validate the multi-mode resonant property as shown in Fig. 7. It can be seen that the frequency locations of the first and the second notched bands move down simultaneously as increase the dimensions of Ls2 and Ls4. And the frequency locations of the second and the third notched bands move down simultaneously as increase the dimensions of Ls1. But only the first the notched band increases as decreases Ls3 and the second notched band increases as decreases Ls5. Therefore, by appropriately adjusting the resonator dimensions, triple notched bands can be achieved at desired frequencies.

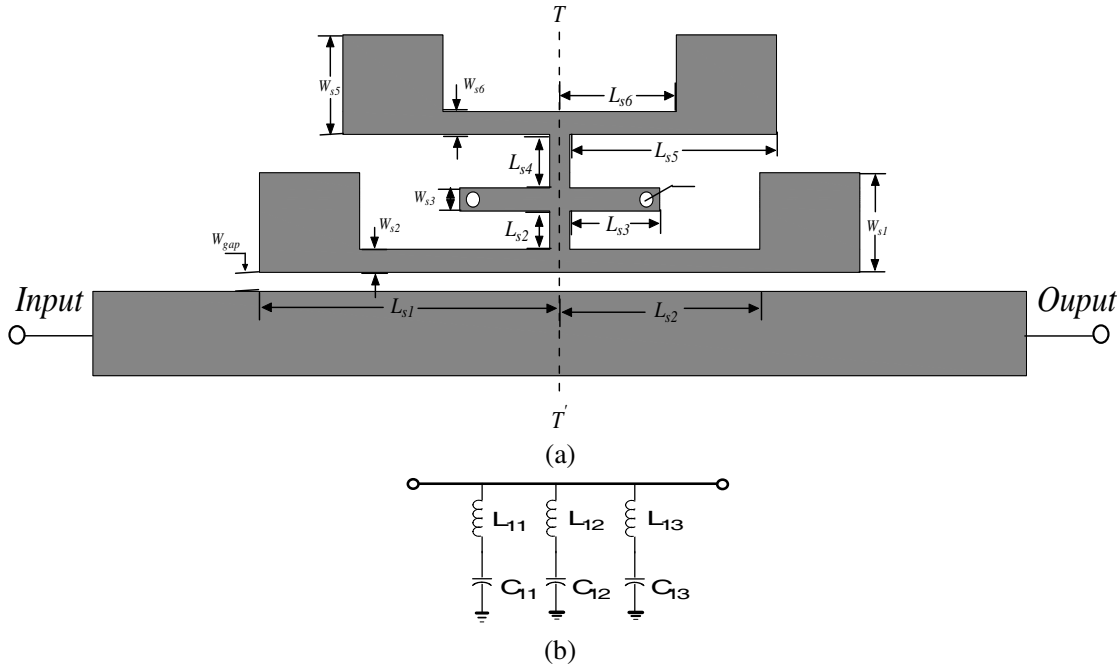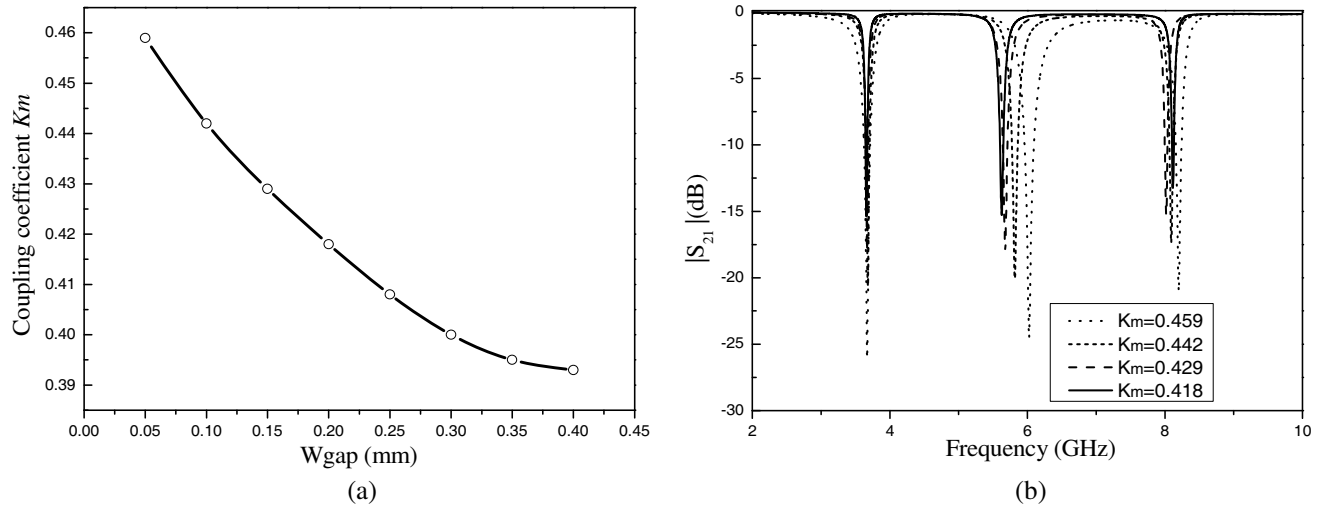**Figure 5.** Geometry and equivalent circuit of the proposed coupled TMSIR.

Figure 6. (a) Simulated coupling coefficient k_m of the coupled TMSIR with different W_{gap}; (b) Simulated S-parameter of the bandwidth of notched bands with different coupling coefficient k_m of the coupled TMSIR.

4. EXPERIMENTAL RESULTS

The designed UWB BPF is measured with an Agilent N5244A vector network analyzer. Fig. 8 shows the comparison between the simulated and measured results. It can be seen that the fabricated UWB BPF has a pass-band from $3.23 \sim 11.06$ GHz as we expected. Three notched bands with respective 3 dB FBWs of 1.9%, 1.4%, and 1.3% are achieved, which ensure a high selectivity for the designed UWB filter. Inside each notched band, the attenuation is better than -10 dB at the center frequencies of 5.2, 6.8, and 8.0 GHz. The minor discrepancy between simulation and measurement results are mainly due
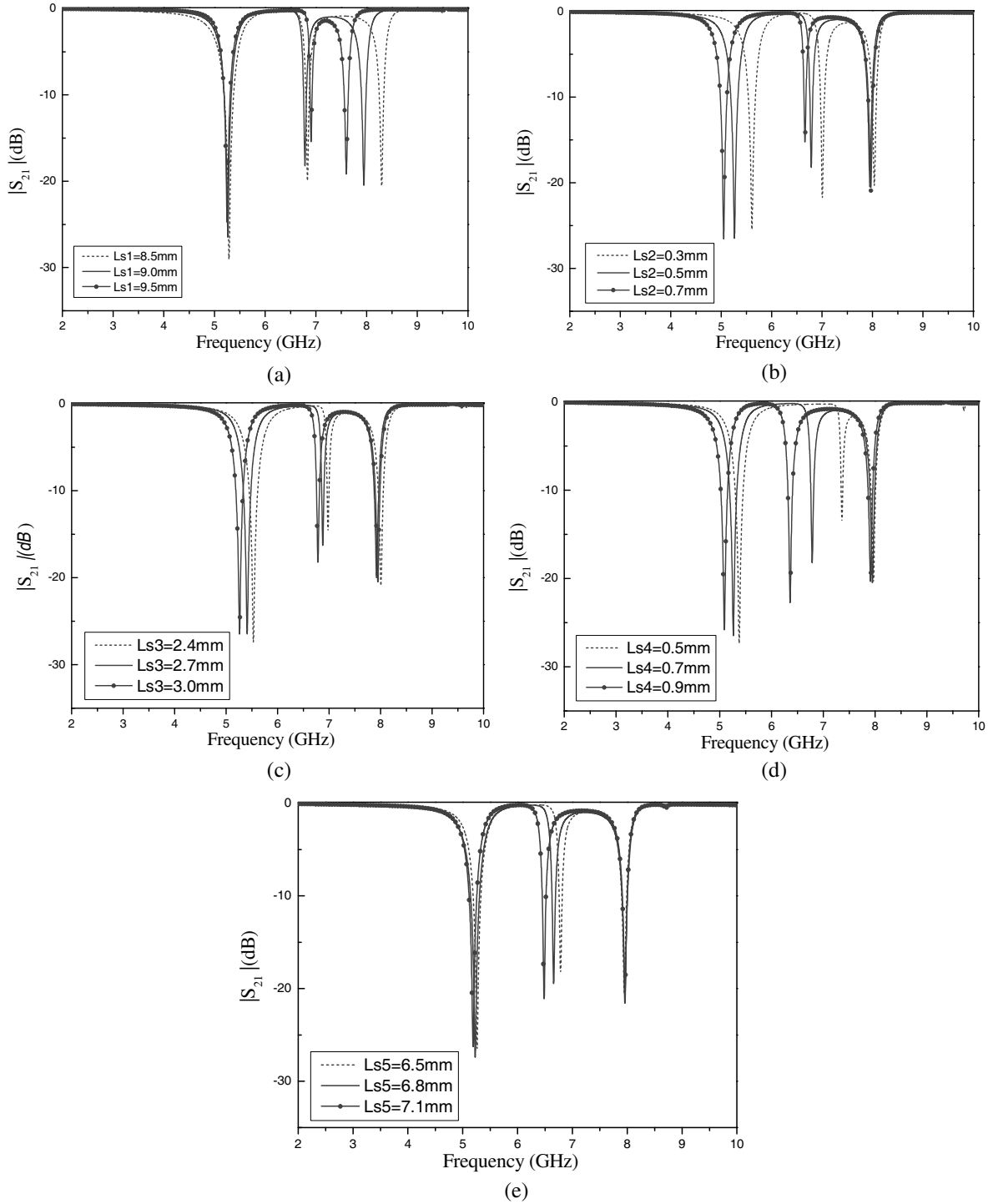
Figure 7. Simulated S-parameters of the coupled TMSIR for various dimensions: (a) LS1, (b) LS2, (c) LS3, (d) LS4, (e) LS5.

to the reflections from the SMA connectors and the finite substrate. Fig. 9 shows the photograph of the fabricated UWB BPF. Comparisons with other reported UWB BPFs with notched bands are listed in Table 3. The proposed triple notched-band UWB BPF in this paper exhibits simple topology, low insertion and high return losses, and low cost.
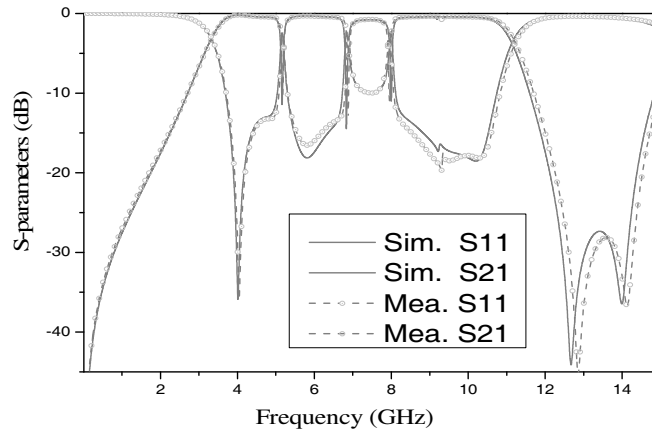
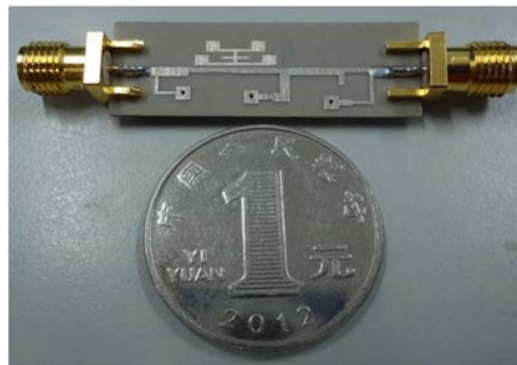**Figure 8.** Simulated and measured S-parameters of the designed UWB BPF.

Figure 9. Photograph of the fabricated UWB BPF with triple-notched bands.

Table 3. Comparisons with other proposed UWB BPF with notched band.

Ref.	Circuit size (λg: at 6.85 GHz)	Circuit dimension	Pass band (GHz)	Insertion loss (dB)	Notch frequency (GHz)/ attenuation (dB)	Upper stop-band (GHz)
[9]	0.81×0.17	2-D	$3.6 \sim 10.2$	0.6	$5.59 > 15$	26
[10]	0.81×0.10	2-D	$3.1 \sim 10.6$	1.0	$5.75 > 20$	12
[11]	1.16×0.68	2-D	$2.8 \sim 10.9$	1.0	$5.85/8.05 > 15$	14
[12]	0.98×0.63	2-D	$3.1 \sim 11.0$	1.0	$5.2/5.8 > 15$	12
[13]	0.53×0.51	3-D	$2.6 \sim 9.6$	1.5	$3.5/5.8 > 15$	11
[14]	1.18×0.26	3-D	$3.2 \sim 10.3$	1.0	$5.38/6.0 > 10$	18
[15]	0.36×0.46	3-D	$2.8 \sim 10$	0.6	$5.23/5.81 > 20$	15
[16]	0.95×0.7	3-D	$4.5 \sim 10.7$	1.5	$5.47/6.05 > 20$	18
[17]	0.88×0.19	2-D	$3.2 \sim 12.0$	1.0	$6.55/8.62 > 20 > 20$	15
[18]	1.27×0.28	2-D	$3.2 \sim 12.4$	1.2	$5.63/6.47/8.93$	16
[19]	2.29×0.69	2-D	$2.5 \sim 10.6$	2.0	$5.57/6.49/9.05 > 15$	12
Our work	1.03×0.38	2-D	$3.1 \sim 10.9$	0.8	$5.2/6.8/8.0 > 10$	15

5. CONCLUSION

A new approach to design compact microstrip UWB bandpass filters with triple band-notched characteristics has been proposed and designed in this paper. The basic UWB BPF is efficiently designed by a variation of genetic algorithm (GA) technique. Then, triple band-notched characteristics are easily generated and realized by controlling the resonance properties of the TMSIR. Good agreement between simulation and measurement results validated the introduced design method. The proposed filter is very useful for modern UWB wireless communication systems due to its distinct properties of simple topology, compact size, and good performance.

ACKNOWLEDGMENT

REFERENCES

1. FCC, "Revision of part 15 of the commission's rules regarding ultra-wide-band transmission system," Tech. Rep., 98–153, ET-Docket, 2002.

2. Zhu, L., S. Sun, and W. Menzel, "Ultra-wideband (UWB) bandpass filters using multiple-mode resonator," *IEEE Microw. Wireless Compon. Lett.*, Vol. 15, No. 11, 796–798, 2005.

3. Wang, H., L. Zhu, and W. Menzel, "Ultra-wideband bandpass filter with hybrid microstrip/CPW structure," *IEEE Microwave Wireless Compon. Letters.*, Vol. 15, No. 12, 844–846, 2005.

4. Shobeyri, M. and M. H. Vadjed-Samiei, "Compact ultra-wideband bandpass filter with defected ground structure," *Progress In Electromagnetics Research Letters*, Vol. 4, 25–31, 2008.

5. Comez-Garcia, R. and J. I. Alonso, "Systematic method for the exact synthesis of ultra-wideband filtering responses using high-pass and low-pass sections," *IEEE Trans. Microw. Theory Tech.*, Vol. 54, No. 10, 3751–3764, 2006.

6. Wong, S. W. and L. Zhu, "Implementation of compact UWB bandpass filter with a notch-band," *IEEE Microw. Wirel. Compon. Lett.*, Vol. 18, No. 1, 10–12, 2008.

7. Wei, F., L. Chen, X.-W. Shi, X. H. Wang, and Q. Huang, "Compact UWB bandpass filter with notched band," *Progress In Electromagnetics Research C*, Vol. 4, 121–128, 2008.

8. Wei, F., Q. Y. Wu, X. W. Shi, and L. Chen, "Compact UWB bandpass filter with dual notched bands based on SCRLH resonator," *IEEE Microw. Wirel. Compon. Lett.*, Vol. 21, No. 1, 28–30, 2011.

9. Wu, H.-W., M.-H. Weng, and C.-Y. Hung, "Ultra wideband bandpass filter with dual notch bands," *Proc. Asia-Pacific Microwave Conf.*, 33–36, Yokohama, Japan, 2010.

10. Hsiao, P.-Y. and R.-M. Weng, "Compact tri-layer ultra-wideband bandpass filter with dual notch bands," *Progress In Electromagnetics Research*, Vol. 106, 49–60, 2010.

11. Hao, Z.-C., J.-S. Hong, S. K. Alotaibi,, J. P. Parry, and D. P. Hand, "Ultra-wideband bandpass filter with multiple notch-bands on multilayer liquid crystal polymer substrate," *IET Microw. Antennas Propag.*, Vol. 3, No. 5, 749–756, 2009.

12. Hao, Z.-C., J.-S. Hong, J.P. Parry, Hand, and D. P. Hand, "Ultra-wideband bandpass filter with multiple notch bands using nonuniform periodical slotted ground structure," *IEEE Trans. Microw. Theory Tech.*, Vol. 57, No. 12, 3080–3088,2009.

13. Luo, X., J.-G. Ma, K. S. Yeo, and E.-P. Li, "Compact ultra-wideband (UWB) bandpass filter with ultra-narrow dual- and quad-notched bands," *IEEE Trans. Microw. Theory Tech.*, Vol. 59, No. 6, 1509–1519, 2011.

14. Nosrati, M. and M. Daneshmand, "Compact microstrip UWB double/single notch-band BPF based on wave's cancellation theory," *IET Microw. Antennas Propag.*, Vol. 6, No. 8, 862–868, 2012.

15. Nosrati, M. and M. Daneshmand, "Developing single-layer ultra-wideband band-pass filter with multiple (triple and quadruple) notches," *IET Microw. Antennas Propag.*, Vol. 7, No. 8, 612–620, 2013.

16. Dong, Y. L., C.-M. Sun, W.-Y. Fu, and W. Shao, "Ultra-wideband bandpass filters with triple and quad frequency notched bands," *Journal of Electromagnetic Waves and Applications*, Vol. 26, Nos. 11–12, 1624–1630, 2012.

17. Hsu, M.-H. and J.-F. Huang, "Annealing algorithm applied in optimum design of 2.4 GHz and 5.2 GHz dual-wideband microstrip line filters," *IEICE Trans. Electronics.*, Vol. E88C, No. 1, 47–56, 2005.

18. Tsai, L.-C. and C.-W. Hsue, "Dual-band bandpass filters using equal-length coupled-serial- shunted lines and Z-transforms technique," *IEEE Trans. Microw. Theory Tech.*, Vol. 52, No. 4, 1111 –1117, 2004.

19. Nicholson, G.-L., and M.-J. Lancaster, "Coupling matrix synthesis of cross coupled microwave filters using a hybrid optimisation algorithm," *IET Trans. Microw. Antennas Propag.*, Vol. 3, No. 6, 1111 –1117, 2009.

20. Zhao, Y.-X., F. Chen, H. Chen, N. Li, Q. Shen, and L. Zhang, "The microstructure design optimization of negative index metamaterials using genetic algorithm," *Progress In Electromagnetics Research Letters*, Vol. 22, 95–108, 2011.

21. Lai, M.-I. and S.-K. Jeng "Compact microstrip dual-band bandpass filters design using genetic-algorithm techniques," *IEEE Trans. on Microwave Theory and Techniques*, Vol. 54, No. 1, Jan. 2006.

22. Gao, L., X. Y. Zhang, B.-J. Hu, and Q. Xue, "Novel multi-stub loaded resonators and their applications to various bandpass filters," *IEEE Trans. Microw. Theory Tech.*, Vol. 62, No. 5, 1162–1172, May, 2014.